A Cross-Layer QoS-Aware Communication Framework in Cognitive Radio Sensor Networks for Smart Grid Applications

Ghalib A. Shah, *Member, IEEE*, Vehbi C. Gungor, *Member, IEEE*, and Ozgur B. Akan, *Senior Member, IEEE*

***Abstract*—Electromagnetic interference, equipment noise, multi-path effects and obstructions in harsh smart grid environments make the quality-of-service (QoS) communication a challenging task for WSN-based smart grid applications. To address these challenges, a cognitive communication based cross-layer framework has been proposed. The proposed framework exploits the emerging cognitive radio technology to mitigate the noisy and congested spectrum bands, yielding reliable and high capacity links for wireless communication in smart grids. To meet the QoS requirements of diverse smart grid applications, it differentiates the traffic flows into different priority classes according to their QoS needs and maintains three dimensional service queues attributing delay, bandwidth and reliability of data. The problem is formulated as a *Lyapunov* drift optimization with the objective of maximizing the weighted service of the traffic flows belonging to different classes. A suboptimal distributed control algorithm (DCA) is presented to efficiently support QoS through channel control, flow control, scheduling and routing decisions. In particular, the contributions of this paper are three folds; employing dynamic spectrum access to mitigate with the channel impairments, defining multi-attribute priority classes and designing a distributed control algorithm for data delivery that maximizes the network utility under QoS constraints. Performance evaluations in *ns-2* reveal that the proposed framework achieves required QoS communication in smart grid.**

***Index Terms*—Cognitive radio sensor networks (CRSNs), cross-layer quality-of-service (QoS), smart grid.**

I. Introduction

SMART grids are recognized as the next-generation power systems, which employ various monitoring and actuating devices to autonomously monitor, diagnose, and control and to efficiently operate the power equipments used in power generation, distribution, and utilization [19], [20]. Recently, wireless sensor networks (WSNs) have been considered as a promising technology to achieve seamless, reliable, and low-cost remote monitoring and control in smart grids [27], [29]. The current and envisioned applications of WSNs in power-grid span a wide range, including advanced metering, remote power system monitoring and control, electricity fraud detection, fault diagnostics, demand response and dynamic pricing, load control and energy management, and power automation [12], [28], [5]. However, the smart grid applications can have different quality-of-service (QoS) requirements and specifications in terms of reliability and communication delay [12], [11], [21]. Recent field tests reveal that wireless links in smart grid environments have higher packet error rates and variable link capacity because of dynamic topology changes, obstructions, electromagnetic interference, equipment noise, multipath effects, and fading [12], [14]. This leads to both time and location dependent delay and capacity variations of wireless links in smart grid environments. Thus, the key design challenges in smart grid are to support reliable and real-time data delivery under adverse transmission conditions [21].

To this end, cognitive radio wireless sensor networks [2] can enhance the overall network performance by dynamic spectrum access and, hence, improve spectrum utilization in smart grid environments [13]. Cognitive radio exploits the temporally unused spectrum, which is defined as a spectrum hole. If a secondary user (SU) encounters the high noise and/or primary user (PU) signal at the particular spectrum band, it migrates to another spectrum hole or stays in the same band without interfering with the licensed user by adapting its communication parameters. In unlicensed spectrum bands, there are no legitimate PUs, and all users have the same right to access the unlicensed spectrum but the use of noisy channels can be prevented. Thus, cognitive radio can be exploited to address the unique challenges of smart grid applications, which are time- and space-varying spectrum characteristics, reliability and latency, harsh propagation conditions, and energy constraints for low-power sensor nodes.

Due to late recognition of smart grids, the research on their communication protocols design is found to be limited. Though QoS routing protocols [16], [25] for smart grid exist but their scope is limited to certain applications, such as price signalling and emergency handling. Similarly, various cross-layer routing protocols [8], [26], [23] are proposed for cognitive radio *ad hoc* networks, which mainly aim to maximize the throughput of SUs under different constraints. A distributed optimization

Manuscript received January 22, 2012; revised June 07, 2012, October 02, 2012, December 28, 2012; accepted January 06, 2013. Date of publication January 23, 2013; date of current version August 16, 2013. This work was supported in part by the EU FP7 Marie Curie International Reintegration Grant (IRG) under Grant PIRG05-GA-2009-249206 and by the Turkish Scientific and Technical Research Council (TUBITAK) under Grant #110E249. Paper no. TII-12-0024.

G. A. Shah is with the Al-Khawarizmi Institute of Computer Science, University of Engineering and Technology, 54000 Lahore, Pakistan.

V. C. Gungor is with the Department of Computer Engineering, Bahcesehir University, 34353 Istanbul, Turkey.

O. B. Akan is with the Next-generation and Wireless Communication Laboratory (NWCL), Department of Electrical and Electronics Engineering, Koc University, 34450 Istanbul, Turkey.

Color versions of one or more of the figures in this paper are available online at http://ieeexplore.ieee.org.

Digital Object Identifier 10.1109/TII.2013.2242083

algorithm is also proposed in [23] that iteratively increases the rate of each flow until it converges to the optimal rate of all of the flows, yet another throughput maximization algorithm. Nevertheless, the existing studies provide optimal solutions to achieve the maximum throughput globally, but they do not consider the needs of each individual flow locally. Particularly, they do not classify the heterogeneous traffic to deal with each traffic class according to its QoS demand. Hence, there exists no cross-layer solution that provides a flexible yet QoS constrained framework for diverse set of applications in a challenging environment.

In this paper, we propose a cross-layer framework that employs cognitive radio communication to circumvent the hostile propagation conditions in power systems and supports QoS for smart grid applications. The proposed framework deals with the channel impairments by dynamically switching among different spectrum bands to seek for a channel with the constrained noise signal. The problem is formulated as a *Lyapunov* drift optimization with the objective of maximizing the weighted service of application flows belonging to different classes. A suboptimal distributed control algorithm (DCA) is presented to efficiently support QoS through dynamic spectrum access, flow control, scheduling, and routing decisions. In DCA, channel selection decision is made dynamically on the basis of perceived signal interference and in turn the estimated channel capacity. Flow control actions are employed to maintain the service of existing flows by confirming the resources availability and adjusting service attributes of newly admitted flows. Similarly, data scheduling and on-demand routing actions are performed to ensure that the data can be delivered to a destination, while preserving its service characteristics. Hence, we present a novel cognitive radio-based cross-layer solution that is tailored to unique characteristics of the power system environment and meets the QoS requirements of smart grid applications. The earlier version of this paper has appeared in [22].

The remainder of this paper is organized as follows. The network model and basic assumptions are described in Section II. The proposed cross-layer framework is presented in Section IV. Performance evaluation results are discussed in Section V. Finally, in Section VI, we draw the main conclusion.

II. Network Model

WSN is a promising technology to achieve seamless, energy-efficient, and reliable remote monitoring and control in smart grid applications. Each sensor node is employed with a cognitive radio interface and is operated through batteries with limited energy source. We assume that the nodes employ single radio that switches among various data channels as well as a predefined control channel, transmitting at a fixed transmission power level P_t. Let $\mathcal{H}_u(t)$ be the set of channels sensed free of PU transmission by a SU u at a time instant t slotted over time slots $\{0, 1, 2, \ldots\}$, with a corresponding interference power set of $\mathcal{I}_u(t) = \{I_u^1, \ldots, I_u^{|\mathcal{H}_u|}\}$. The time-varying capacity achieved on each of these channels is $\mathcal{B}_u(t) = \{b_u^1, \ldots, b_u^{|\mathcal{H}_u|}\}$ that can be computed using Shannon capacity formula.

TABLE I
Smart Grid Applications and Their QoS Specifications [11]

Application	β (kbps)	τ (sec)	α (%)
Smart metering (AMI)	14-100	2	99-100
Price signalling	9.6-56	2	99
Automated feeder switching	9.6-56	1-2	99
Demand Response	56	2	99-100
Emergency Response	40-250	0.5	99-100
Residential energy management	9.6-56	1	90
Building automation	16-32	1-2	90
SCADA	56-100	2-5	99
Distributed generation	9.6-56	2	99
Distributed management & control	56	2	99
Overhead transmission line monitoring	9.6-64	1	90
Outage management	56	2	99

TABLE II
Definition of the Variables Used in the Model, Which Are Observed at Time Slot t

Symbol	Description
$b_u^h(t)^+$	Surplus bandwidth at node u using channel h.
$\bar{\tau}_{\vec{uv}}$	Average link delay between node u and v.
$\beta_i(t)$	Application data rate of flow i.
$\beta_i^c(t)$	Application data rate of flow i of class c.
$\widetilde{\beta}_i^c(t)$	Actual data rate of flow i of class c.
$\beta_{uv}^c(t)$	Application data rate of class c flows at node u to pass through the forwarding node v.
$\widetilde{\beta}_{uv}^c(t)$	Actual data rate of class c flows at node u to pass through the forwarding node v.
$d_u^c(t)$	The dropped data due to reliability tolerance of class c by node u.
$\bar{b}_u^h(t)$	Mean bandwidth using channel h by node u.
$\lambda_u^c(t)$	The total arrival rate of class c at node u.
λ_{max}^c	Maximum arrival rate of flows of class c.
$\mathcal{P}_i$	Path of flow i towards the destination sink.

A. Smart Grid Applications and QoS Requirements

To efficiently operate the smart grids [24], the required information can be provided to utilities by sensor systems to enable them achieving dynamic power management. WSN-based smart grid applications are described in detail in [11] along with their diverse QoS requirements. For example, distributed feeder automation applications require low-latency and high-data-rate communications among substations and intelligent electronic devices in order to timely detect and isolate faults. On the other hand, smart metering applications require latency-tolerant information exchange between the meters and utility management center. Table I summarizes the most important applications and their QoS specifications attributed in terms of data rate (β), delay (τ), and reliability (α), which can be mapped to the traffic classes described in Section V. Nevertheless, the list of applications is momentary and the introduction of new applications do not affect the functioning of the proposed solution since the flexibility of traffic classes allow them to accommodate easily.

To model the smart grid traffic, let $\mathcal{C}$ be the set of priority classes and $\Omega = \{\omega_1, \ldots, \omega_{|\mathcal{C}|}\}$ be the set of weights assigned to them for prioritizing. Each class is attributed by QoS parameters β, τ and α. A class $c \in \mathcal{C}$ has a priority weight $\omega_c \in \Omega$ and is bounded to some minimum and maximum threshold values for these attributes $\{(\beta^c_{\min}, \beta^c_{\max}), (\tau^c_{\min}, \tau^c_{\max}), (\alpha^c_{\min}, \alpha^c_{\max})\}$. The threshold interval of each attribute corresponds to the tolerance of the attribute in a class. Similarly, there may exist an arbitrary number of flows in each class such that $F_c(t)$ is the set of flows in class c at time slot t and the set of flows $\mathcal{F}$ present in the entire network is, $\mathcal{F} = \cup_{c\in\mathcal{C}} F_c$. Hence, the ith flow of class c is privileged to use the respective service, where $\beta^c_{\min} \le \beta_i \le \beta^c_{\max}, \tau^c_{\min} \le \tau_i \le \tau^c_{\max}$ and $\alpha^c_{\min} \le \alpha_i \le \alpha^c_{\max}$.

In order to express the utility of a particular application on achieving its desired QoS, a utility function is defined. When the application specifies its delay requirement to achieve benefit, its utilization depends on the probability that the delay is achieved by the network. For instance, demand response management application sets its communication delay to keep the demand and supply balanced otherwise it would cost in terms of excessive energy production or shortage. The similar notion is applied to the reliability and bandwidth utility. Let $U_u(\beta_i)$, $U_u(\tau_i)$, and $U_u(\alpha_i)$ represent the utility at meeting data rate, delay and reliability requirement of flow i passing through node u at time t. The utility function for the communication parameters is computed as

$$U^c_u(\beta_i, \tau_i, \alpha_i) = \omega^\beta_c U_u(\beta_i) + \omega^\tau_c U_u(\tau_i) + \omega^\alpha_c U_u(\alpha_i) \quad (1)$$

where the weighting coefficients ω^β_c, ω^τ_c, and ω^α_c intensify each of the QoS parameters in a class separately and $\omega_c = \omega^\beta_c + \omega^\tau_c + \omega^\alpha_c$. ω_c is translated to explicit application utility in terms of benefit or profit on achieving appropriate network service.

B. Problem Definition

We formulate a problem, whose objective is to maximize the utility of the node u through its downstream node v subject to the data rate, latency and reliability constraints as

$$\textbf{Maximize}: \quad \sum_{c\in C}\sum_{i\in F_u} U^c_u(\beta_i, \tau_i, \alpha_i), \forall u \in \mathcal{N} \quad (2)$$

$$\textbf{Subject to}: \quad \beta_i \le b^h_u(t)^+, \quad h \in \mathcal{H}_u \cap \mathcal{H}_v, \vec{uv} \in \mathcal{P}_i \quad (3)$$

$$\sum_{j=1}^{|\mathcal{P}|} x^h_j(t) = 0$$

$$j \ne i, \forall\, \vec{yz} \in \mathcal{P}_j, (y,z) \in \mathcal{N}_u \cup \mathcal{N}_v, \vec{uv} \in \mathcal{P}_i \quad (4)$$

$$\sum_{\vec{uv}\in\mathcal{P}_i} \bar{\tau}_{\vec{uv}} \le \tau_i \quad (5)$$

$$\alpha_i \ge \alpha^c_{\min} \quad (6)$$

where x^h_u is the channel control variable that takes the value 1 if the channel h is selected by u, and 0 otherwise.

In the above formulation, constraint (3) ensures that a flow is admitted only when its data rate requirement can be satisfied through the surplus capacity $(b^h_u(t)^+)$ on the selected channel while the existing flows continue to be served. Constraint (4) prohibits the use of same channel by any of the neighbors of sender or receiver at the same time t, while constraint (5) corresponds to the selection of a path that can deliver the data within the given flow delay. Similarly, constraint (6) makes sure that the reliability of the channel in terms of bit error rate (BER) is higher than the reliability demanded by the flow.

III. Lyapunov Drift Optimization

To solve the utility maximization problem, we apply Lyapunov optimization techniques. Prior works [15], [10], [18] on stochastic network optimization provide a detailed methodology for minimizing the Lyapunov drift of not only physical queue backlogs in a queuing network, but also virtual queues introduced to constrain other system resources. To solve the problems (2)–(6), we first transform all of the constraints into queue stability problems. It follows that if we can design a control algorithm that makes all actual queues and virtual queues mean rate stable, and yields maximum utility for smart grid applications, then the problems (2)–(6) are solved. In the following section, we define the physical queues and the virtual queues with their update functions. The distributed control algorithm is presented in Section IV to achieve stability in the queues. We define physical queue Q to represent the routing queue backlog, and virtual queues G, H and Z for Constraints 2, 3 and 5, respectively. Whereas, the stability of G and H jointly ensures constraint (6).

Each network node u maintains a set of output priority queues and determines the forwarding node v on the path. Representing $\mathbf{a}(t) = (a_1, \ldots, a_{|\mathcal{F}|})$ as the vector of data that arrives to the transport layer for each flow on slot t. We assume that a transport layer flow controller observes $a_i(t)$ for ith flow every slot and decides how much of this data to add to the network layer at its source node and how much to drop. Flow control decisions are made to limit queue buffers and ensure the network stability. Such an adaptive flow controller exploits the reliability tolerance of the flows in their admission. Let $(\beta_i(t))|^{\mathcal{F}}_{i=1}$ be the collection of flow control decision variables on slot t. These decisions are made subject to the flow control constraint $0 \le \beta_i(t) \le a_i(t)$. If the flow is rejected, then $\beta_i(t) = 0$, otherwise $\beta^c_{\min} \le \beta_i(t)$ for a minimum data rate $\beta^c_{\min}$ of a flow of class $c \in C$.

Let $Q_u(t)$ denote the matrix of current weighted queue backlogs at node u, where $Q_u(t) = 0$ at $t = 0$. Denote $\mathcal{F}^c_u \subseteq \mathcal{F}$ as the set of flows of class c at the source node u and $Q^c_u(t)$ the queue backlog of class $c \in C$ type queue. The change in queue backlog after slot t is computed as

$$Q^c_u(t+1) = Q^c_u(t) - \sum_{v\in\mathcal{N}_u} \beta^c_{uv}(t) + \sum_{w\in\mathcal{N}_u} \tilde{\beta}^c_{wu}(t) + \sum_{f_i\in\mathcal{F}^c_u} \beta^c_i(t)$$

where $\tilde{\beta}^c_{uv}(t) \le \beta^c_{uv}(t)$, due to the potentially dropped data $d^c_u(t)$ and, therefore, we have $\tilde{\beta}^c_{uv}(t) \triangleq \beta^c_{uv}(t) - d^c_u(t)$ for

$0 \le d_u^c(t) \le (1-\alpha_{\min}^c) \times |Q_u^c(t)|$. We also define the total incoming traffic of class c at node u as

$$\lambda_u^c(t) \triangleq \sum_{w\in\mathcal{N}_u} \tilde{\beta}_{wu}^c(t) + \sum_{i\in F_u^c} \beta_i^c(t).$$

If there is not enough data to send at the offered rate or higher priority queue is served then null data is sent, so that

$$Q_u^c(t+1) = \max\left[Q_u^c(t) - \sum_{v\in\mathcal{N}_u} \beta_{uv}^c(t), 0\right] + \lambda_u^c(t). \quad (7)$$

To satisfy constraint (3), we define a virtual queue $G_u^c(t)$ [18] at node u for traffic class $c \in C$ that represents the queue drain on the channel h of a link originated at u and is changed as

$$G_u^c(t+1) = \max\left[G_u^c(t) + b_u^h(t)^+ + d_u^c(t) - \beta_i^c(t), 0\right]. \quad (8)$$

Now, if $Q_u^c(t) \le G_u^c(t)$, then the flow request is accepted, otherwise rejected. If both the queues are stable, then it yields

$$\lambda_u^c(t) - \sum_{v\in\mathcal{N}_u} \beta_{uv}^c(t) \le b_u^h(t)^+ + d_u^c(t) - \beta_i^c(t).$$

Rearranging the above, we obtain

$$\tilde{\beta}_i^c(t) + \lambda_u^c(t) - \sum_{v\in\mathcal{N}_u} \beta_{uv}^c(t) \le b_u^h(t)^+.$$

If a node has surplus capacity at its forwarding link (u, v), i.e., $b_u^h(t)^+ \ge 0$, then we have $\lambda_u^c(t) - \sum_{v\in\mathcal{N}_u} \beta_{uv}^c(t) = 0$. Hence, a flow at rate $\tilde{\beta}_i^c(t)$ with its loss tolerance is admitted satisfying constraint (3).

Similarly, we define a virtual queue $H_u(t)$ for a channel selection, which is initialized to 0, i.e., $H_u(0) = 0$. The number of nodes using the free channel $h \in \mathcal{H}_u$ to be used at the link (u, v) at any time t is $H_u(t) \ge 0$. The nodes selecting channel h cannot be negative, and, therefore, we always have $\sum_{w\in\mathcal{N}} x_w^h \ge 0, \forall h \in \mathcal{H}$. Thus, the queue is updated as

$$H_u(t+1) = H_u(t) + \sum_{w\in\mathcal{H}_u\cup\mathcal{H}_v} x_w^h(t). \quad (9)$$

Constraint (4) is satisfied subject to the stability of the virtual queue $H_u(t)$ at time t.

To ensure the worst-case delay is bounded, we define a virtual queue $Z_u^c(t)$ at node u for $c \in C$ with $Z_u^c(0) = 0$ that is updated as

$$Z_u^c(t+1) = \max\left[Z_u^c(t) - \sum_{v\in\mathcal{N}_u} \beta_{uv}^c(t) - d^c(t) + \lambda_u^c(t), 0\right]. \quad (10)$$

The bound $\lambda_{\max}^c$ on maximum arrival rate of class c limits its number of flows as $F_u^c \le \lambda_{\max}^c/\beta_{\min}^c$. The size of $Z_u^c(t)$ provides a bound on the delay of the head-of-queue data in queue $Q_u^c(t)$ in a FIFO scheduling. If a scheduling algorithm ensures that $Z_u^c(t) \le Z_{\max}^c$ and $Q_u^c(t) \le Q_{\max}^c$ for all t and finite constants $Z_{\max}^c$ and $Q_{\max}^c$ for a class c flows, then the worst-case delay $\tau_{\max}^c$ is obtained [18] as

$$\tau_{\max}^c = \left\lceil \left(Q_{\max}^c + Z_{\max}^c\right)/\lambda_{\max}^c \right\rceil. \quad (11)$$

We use Lyapunov drift optimization for stable queue scheduling [18] in order to make transmission decision based on channel states and the current queue backlogs maintained separately for each traffic class. Define $\mathbf{\Theta(t)} \triangleq [Q(t); G(t); H(t); Z(t)]$ and a non-negative Lyapunov function for set of queues of $c \in \mathcal{C}$ at node u as

$$L_u(\mathbf{\Theta}_u(t)) \triangleq \frac{1}{2}\left[Q_u^c(t)^2 + G_u^c(t)^2 + H_u(t)^2 + Z_u^c(t)^2\right]. \quad (12)$$

Now we define $\Delta\mathbf{\Theta}_u(t)$ as the conditional Lyapunov drift at node u and minimize a bound on the following drift-minus-utility at every node independently as

$$\begin{aligned}
&\Delta\mathbf{\Theta}_u(t) - V\mathbb{E}\left\{U_u^c\left(\mathcal{F}_u^c(t)\right) \mid \mathbf{\Theta}_u(t)\right\} \\
&\quad \le B + \mathbb{E}\left\{Q_u^c(t)\left[\lambda_u^c(t) - \sum_{v\in\mathcal{N}_u}\beta_{uv}^c(t)\right]\middle|\mathbf{\Theta}_u(t)\right\} \\
&\qquad + \mathbb{E}\left\{H_u(t)\sum_{w\in\mathcal{H}_u\cup\mathcal{H}_v} x_w^h(t)\middle|\mathbf{\Theta}_u(t)\right\} \\
&\qquad + \mathbb{E}\left\{G_u^c(t)\left[b_u^h(t)^+ - \tilde{\beta}_i^c(t)\right]\middle|\mathbf{\Theta}_u(t)\right\} \\
&\qquad + \mathbb{E}\left\{Z_u^c(t)\left[\lambda_u^c(t) - \sum_{v\in\mathcal{N}_u}\tilde{\beta}_{uv}^c(t)\right]\middle|\mathbf{\Theta}_u(t)\right\} \\
&\qquad - V\mathbb{E}\left\{U_u^c\left(\mathcal{F}_u^c(t)\right)|\mathbf{\Theta}_u(t)\right\} \quad (13)
\end{aligned}$$

where V is a control parameter chosen to tradeoff between the utility and relaxing constraints, and B is a bound defined as

$$\begin{aligned}
B \ge \frac{1}{2}\Bigg[&\mathbb{E}\left\{\left(\lambda_u^c(t)^2 + \sum_{v\in\mathcal{N}_u}\beta_{uv}^c(t)^2\right)\right\} \\
&+ \mathbb{E}\left\{\left(b_u^h(t)^+ - \tilde{\beta}_i^c(t)\right)^2\right\} \\
&+ \mathbb{E}\left\{\sum_{w\in\mathcal{H}_u\cup\mathcal{H}_v} x_w^h(t)^2\right\} \\
&+ \mathbb{E}\left\{\left(\lambda_u^c(t) - \sum_{v\in\mathcal{N}_u}\tilde{\beta}_{uv}^c(t)\right)^2\right\}\Bigg].
\end{aligned}$$

Any algorithm that minimizes the drift in (13) results in system queues, which is a constant multiple of the optimal utility in worst case. To achieve this, we employ a distributed control algorithm since the global solution is NP-hard and is not efficient for resource constrained devices.

IV. Distributed Control Algorithm (DCA)

The DCA minimizes the right-hand side of the inequality (13) for each node by making the channel decision, flow control decision, packet dropping, or reliability decision. Therefore,

the problem in (13) is decomposed into three separable subproblems related to each control action. The channel selection problem in DCA is solved to maintain an optimal link state for routing. Although flow control can be solved independently but its solution is based on the input obtained from the channel control action. Similarly, packet scheduling and dropping problem takes input from the flow control and channel decisions but its solution is independent to these problems as described in Section IV-C. Hence, the overall solution in DCA is obtained through cross-layer interaction and solution of its subproblems. Since all the arrivals and transmission decisions are independent of the queues backlog, we can omit the condition of $\mathbf{\Theta}_u(t)$ in the expectations in (13). For every slot t, a node u observes the physical queue $Q_u^c(t)$ for each class $c \in \mathcal{C}$ and the virtual queues $G_u^c(t)$, $H_u(t)$, and $Z_u^c(t)$ and performs the actions in the following control phases.

A. Channel Control

Let the node u select the channel $h^* \in \mathcal{H}_u$, i.e., $x_u^{h^*}(t) = 1$. The channel control problem is then formulated as

$$\begin{aligned} \textbf{minimize}: \quad & H_u(t) \sum_{w \in \mathcal{H}_u \cup \mathcal{H}_v} x_w^{h^*}(t) \\ \textbf{subject to}: \quad & 0 \le y_{uv}^{h^*} \le 1, v \in \mathcal{N}_u \\ & p_u^{\alpha}(h^*) \ge \alpha_{\min}^c. \end{aligned}$$

In order to solve the above, a routing algorithm makes the decision $y_{uv}^{h^*}$ by choosing the forwarding node v and selects the channel h^* in neighborhood of both u and v that minimizes saturation $(\rho_u^{h^*}(t))$ in the vicinity of u to avoid interference. The probability of channel selection is computed as

$$\psi_u^{h^*}\left(I_u^{h^*}(t), \rho_u^{h*}(t)\right) = 1 - \frac{1}{2}\left(\frac{I_u^{h*}(t)}{\max_{g \in \mathcal{H}_u}\{I_u^g\}} + \frac{\rho_u^{h*}(t)}{|\mathcal{N}_u|}\right).$$

The necessary condition in selecting h^* is the BER that should not exceed the tolerance of a flow of class $c \in C$ to ensure the constraint (6). Thus, $x_u^{h^*}(t)$ takes the value as

$$x_u^{h^*}(t) = \begin{cases} 1, & \text{if } p_u^{\alpha}(h^*) \ge \alpha_{\min}^c \\ & \wedge \psi_u^h(t) \ge \max_{g \in H_u}\{\psi_u^g(t)\} \\ 0, & \text{otherwise} \end{cases} \tag{14}$$

where $p_u^{\alpha}(h^*)$ is the BER computed for channel h^* based on its noise signal $I_u^{h^*}$. This is achieved by using a CSMA-based MAC protocol in which the structure of frame is composed of three periods; spectrum sensing (SS) period $T_{\rm ss}$, control (CTRL) period $(T_{\rm ctrl})$ and data transmission (DATA) period (T_{tx}). Notably, the frame period is of fixed duration $\mathcal{T}$ but its distribution into three periods is variable. At the beginning of each frame, spectrum sensing [3] is performed for a period of $(T_{\rm ss} = |\mathcal{H}| \times \delta \times \theta)$ *sec*, where δ is the basic slot period and θ is the maximum number of slots to sense a channel. After obtaining a list of free channels, MAC initiates the control period that may span over $\mathcal{T} - T_{\rm ss}$ initially but skews to its minimum length $T_{\rm ctrl}^{\min}$ as the data request is received or generated. Similarly, the transmission period is initially set to 0 but is stretched to $\mathcal{T} - T_{\rm ss} - T_{\rm ctrl}$ for data transmission. If no data transmission takes place for a number of idle frames threshold then it resets both to initial values.

For data transmission, node u sends channel contention request to its potential receiver v that contains the list of channels with the preferred channel $h \in \mathcal{H}_u$ marked. u also determines the saturation on each channel that it overhears and makes the selection decision using (14). Likewise, v computes the channels selection probability and sends the response back with the selection $h^* \in \mathcal{H}_u \cap \mathcal{H}_v$ to u. If $h \in \mathcal{H}_v$ and the interference is also tolerable then v prefers to use it, i.e., $h^* = h$, otherwise it replies with its own preferred channel, i.e., $h \ne h^*$. However, u is obliged to use h^* and confirms it by sending acknowledgment. Thus, all of the neighbors of the sender and receiver will be aware of the usage of h^* during the current frame that evades interference by other SU nodes.

B. Admission Control

Each node u makes the flow admission decision to solve

$$\begin{aligned} \textbf{minimize}: \quad & \sum_{c \in \mathcal{C}} \sum_{i \in \mathcal{F}_u^c} G_u^c(t)\left[b_u^h(t)^+ - \beta_i^*(t)\right] \\ & - V U_u^c(\beta_i, \tau_i, \alpha_i) \\ \textbf{subject to}: \quad & 0 \le \beta_i^*(t) \le \beta_{\max}^c. \end{aligned}$$

A node selects the amount $\beta_i^*(t) \le \beta_i(t)$ of each flow that minimizes the surplus capacity of the link and eventually maximizes the utility of the flows scaled by factor V. The throughput utility of a flow is computed as $(1 - b_u^h(t)^+ / b_u^h(t))$. Thus, a flow utilizing more capacity gets higher utility value. Moreover the utility is weighted by its class priority as given in (1) that motivates to prioritize the flows of higher priority class for maximizing the utility. To achieve this, we implement a *high-priority-low-rate* algorithm that allows to admit the large number of low rate flows of high priority class that eventually minimizes the surplus capacity and significantly maximizes the utility. Consider two flows i and j competing at node u to be admitted belonging to classes $c \in \mathcal{C}$ and $c^* \in \mathcal{C}$, respectively. Now, if $(\beta_i + \beta_j) \le b_u^h(t)^+$, then the admission controller allows both of them to enter the network layer such that $\beta_i \le \beta_{\max}^c$ and $\beta_j \le \beta_{\max}^{c^*}$. On the other hand, if $(\beta_i + \beta_j) > b_u^h(t)^+$, then it selects the flow of higher priority class and admits i if $\omega_c > \omega_{c^*}$, otherwise j is admitted. However, if $\omega_c = \omega_{c^*}$, then it chooses the flow whose data rate is lower. In the worst case, if $\beta_i > b_u^h(t)^+$, it exploits the reliability tolerance to adjust the flow rate under the capacity constraint. Therefore, it drops a fraction of the data to reduce the offered rate $\widetilde{\beta}_i \le \beta_i$, where the new data rate is $\widetilde{\beta}_i = (1 - (\alpha_i - \alpha_{\min}^c)) \times \beta_i$ and admits the flow if $\widetilde{\beta}_i > b_u^h(t)^+$, otherwise it rejects.

C. Delay Control

Let $z_{uv}^{c^*}$ be the binary variable that takes the value 1 if the flow of class c is scheduled for transmission on link $\overrightarrow{uv}$, otherwise 0.

To satisfy the constraint (5), each node makes the scheduling and routing decision to solve the following problem:

$$\begin{aligned}\textbf{minimize}: \quad & \sum_{c\in\mathcal{C}}\sum_{f_i\in\mathcal{F}_u^c}\left[Q_u^c(t)\left[\lambda_u^c(t)-\sum_{v\in\mathcal{N}_u} z_{uv}^{c^*}\beta_{uv}^c(t)\right]\right. \\ & \left.+Z_u^c(t)\left[\lambda_u^c(t)-\sum_{v\in\mathcal{N}_u} z_{uv}^{c^*}\tilde{\beta}_{uv}^c(t)\right]\right] \\ & -VU_u^c(f_i(\beta_i,\tau_i,\alpha_i)) \\ \textbf{subject to}: \quad & |\mathcal{P}_i|\le\mathcal{P}_L, \mathcal{P}_i\in\mathcal{P}.\end{aligned}$$

The minimization objective is achieved by reducing the data stored in queues, that is, schedule as much data as possible for transmission during the current frame to minimize the backlogged data. At the same time, the delay utility is also required to be maximized, which is best achieved by selecting the high priority class and the critical delay flow. We devise a *high-priority-critical-delay* algorithm for scheduling data from different queues. For each class $c\in\mathcal{C}$, node u drops the data of ith flow exceeding its delay limit since it might cause delay in transmission of other data packets. Therefore, it drops if

$$\frac{|Q_u^c(t)+Z_u^c(t)|}{\bar{\lambda}_u^c(t)}>\frac{\tau_i}{|\mathcal{P}_i|}.$$

Otherwise, selects the queue for scheduling whose product of delay weight and criticality is the highest among all the queues. It then computes the queue scheduling variable as

$$\zeta_u^c(t)=\omega_c^{\tau}\times\frac{|Q_u^c(t)+Z_u^c(t)|}{\bar{\lambda}_u^c(t)}\times\frac{|\mathcal{P}_i|}{\tau_i}.$$

Thus, the scheduling control variable is defined as

$$z_{uv}^{c^*}(t)=\begin{cases}1 & \text{if } \zeta_u^{c^*}(t)\ge\max_{c\in\mathcal{C}-\{c^*\}}\{\zeta_u^c(t)\}\\ 0 & \text{otherwise}\end{cases} \tag{15}$$

The control algorithm schedules the packets from different classes that limits the queue size to minimize the delay as given in (11). Moreover, the routing algorithm ensures the route length to the maximum path length, which is possibly a shortest routing path. However, if there are many feasible paths from source to destination then it does not necessarily select the shortest rather incorporates load balancing to avoid congestion and eventually achieves the reliability.

A route length threshold $\mathcal{P}_L$ is defined to limit the number of hops for each source. The worst case end-to-end delay is obtained by $\mathcal{P}_L\times\tau_{\max}^c$ that bounds the delay of ith route as

$$\sum_{\vec{uv}\in\mathcal{P}_i}\tau_{\vec{uv}}^c\le\mathcal{P}_L\times\tau_{\max}^c,\ \forall\mathcal{P}_i\in\mathcal{P}.$$

V. Performance Evaluation

Here, we present the performance results of the proposed DCA framework simulated using *ns-2* [30]. To simplify the evaluation, we consider four different classes of applications;

TABLE III
Traffic Classes With Their Attribute Values

Class	ω	β_{min} (kbps)	β_{max} (kbps)	τ_{min} (sec)	τ_{max} (sec)	α_{min} (%)	α_{max} (%)
XRtX	1/7	16	20	0.25	0.75	N/A	N/A
HRaRtX	3/7	32	40	1	2	N/A	N/A
RaRtRe	2/7	20	28	0.5	1	90	100
RaXRe	1/7	10	28	N/A	N/A	90	100

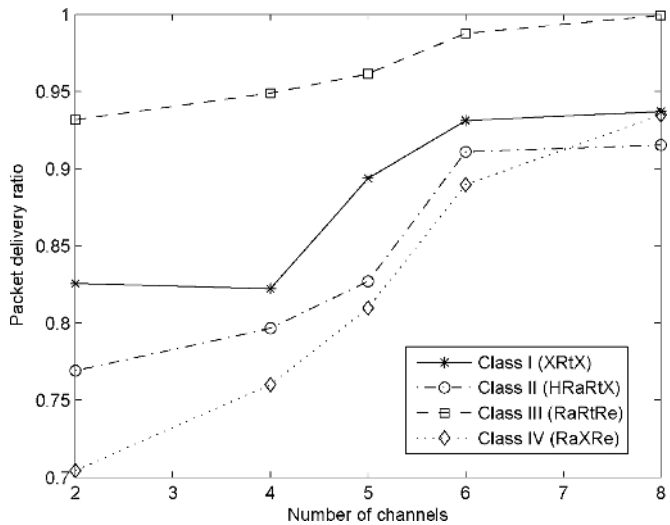

Fig. 1. Average packet delivery ratio representing the reliability for flows of different traffic classes at varying number of cognitive channels.

Class I: real-time critical (*XRtX*), e.g., emergency response, Class II: real-time and high data rate (*HRaRtX*), e.g., automated demand supply, Class III: certain data rate, reliability and real-time constraints (*RaRtRe*), e.g., SCADA, and Class IV: certain data rate and reliability (*RaXRe*), e.g., smart metering. The QoS specifications of these classes are listed in Table III. The performance metrics are reliability, packet latency, and data rate. The impact on these evaluation parameters is investigated by varying the number of flows of different classes with the number of channels upto eight. PUs also appear on the channels to induce unwanted interference and limit the access of the given spectrum. The total number of sensor nodes are 49 deployed in 7×7 grid with the sink chosen at the corner of the grid. Due to lack of QoS routing framework in CRSN, we compare the performance with MMSPEED [9] proposed for WSN to give an insight to the benefit of using cognitive radio in a hostile environment.

In the first scenario, there are five flows per each class, for the four traffic classes to report the reliability results under high network load with high data rate demands. PUs are present on the first four channels but the sensor nodes still switch among all the channels to mitigate the interference. It can be seen in Fig. 1 that the reliable class *XRtRe* maintains higher delivery ratio of 95% approximately even at the smaller number of channels but approaches to almost one as the number of channels are sufficient to create more transmission opportunity. However, other

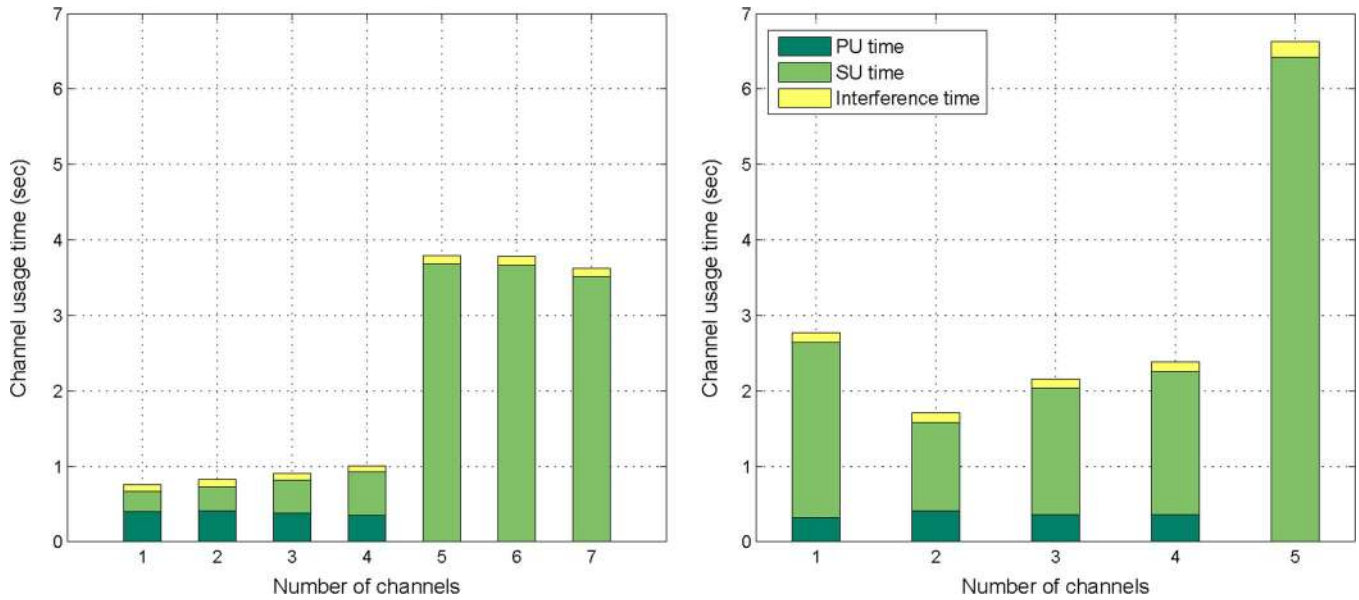

Fig. 2. Channel usage in the proposed framework.

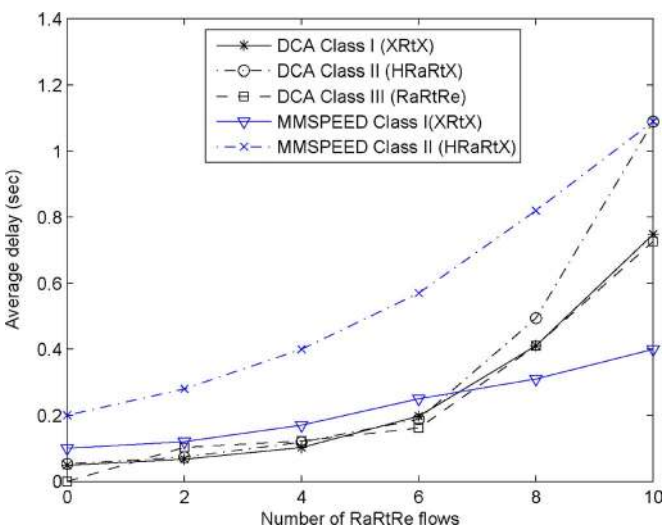

Fig. 3. Average packet delay for five class *XRtX* flows, five class *HRaRtX* flows, and a varying number of class *RaRtRe* flows.

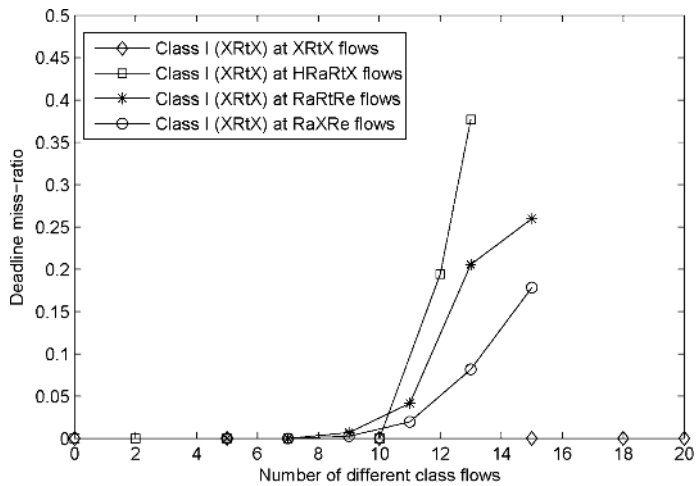

Fig. 4. Packet deadline miss-ratio for flows of real-time class *XRtX* at delay bound of 0.6 s by increasing the number of flows for each class.

classes could not achieve that higher reliability since their reliability attribute is set to lower. Class *XRtX* also achieves the reliability upto 95% at eight channels, but other classes do not reach that level even by increasing the number of channels. This is due to the fact that the single common control channel becomes the bottleneck for large number of contenders to negotiate data channels. In order to visualize the fundamental of achieving reliability in a hostile environment by using cognitive radios, Fig. 2 demonstrates the usage of the channels. Since PUs are present only on the first four channels, it is clear that SUs mainly utilize the channels above four, which have lesser interference from PUs or noise. Therefore, the interference with the PUs is reported under the 10% of the channel usage time. This clearly proves the effectiveness of cognitive radios in smart grid systems.

In the second scenario, we evaluate the real-time support by reporting average packet delay for the real-time classes *XRtX*, *HRaRtX*, and *RaRtRe* at the deadline of 0.6 s. We initiate five flows for the *XRtX* and *HRaRtX* classes and increase the number of flows of other two classes. Fig. 3 illustrates the impact of varying the number of class *RaRtRe* flows up to 10. Clearly, the three real-time classes meet their deadlines until the flows were increased to 9, but the delay starts increasing exponentially as the number of flows reaches 10. However, the delay increase for the highest priority class *XRtX* is smaller than the others, while it is significantly larger for the second priority class *HRaRtX* due to its high data rate than the remaining two classes. The delay performance is also compared with MMSPEED [9] that exploits multipath routing and achieves low delay in data routing according to the priority of class. It can be observed that the difference of delay between the lower priority class II and higher priority class I is notable in MMSPEED that eventually

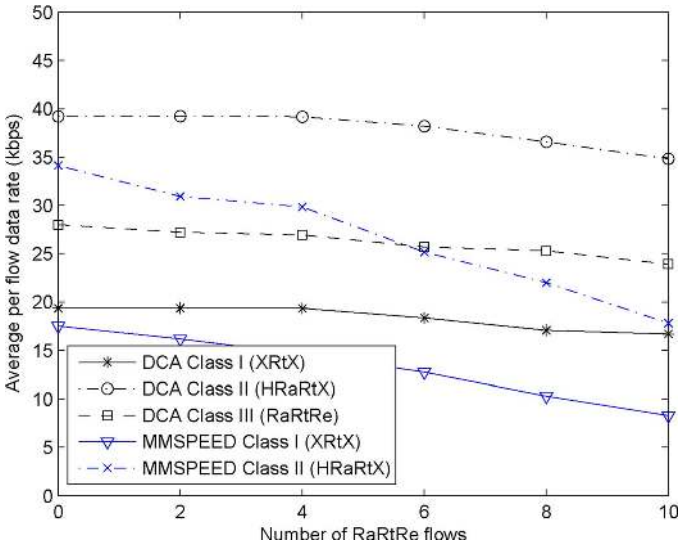

Fig. 5. Average data rate for five class *XRtX* flows, five class *HRaRtX* flows, and varying number of class *RaRtRe* flows.

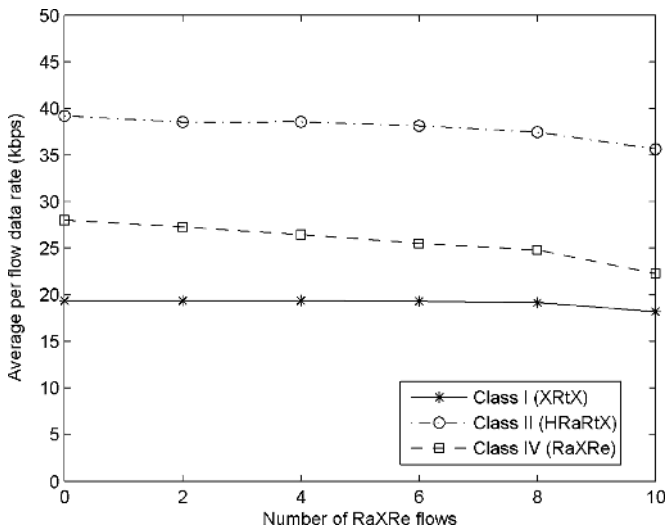

Fig. 6. Average data rate for five class *XRtX* flows, five class *HRaRtX* flows, and varying number of the lowest priority class *RaXRe* flows.

does not scale to defining more priority classes for increased and diverse applications of smart grids. To further elaborate the latency performance, Fig. 4 shows the deadline miss ratio for class *XRtX*, which reflects the same trend as discussed for the average packet delay.

In Fig. 5, the impact on data rate of first three classes is presented by varying the number of flows of class *RaRtRe*. At higher load under ten additional flows, the data rate provided to class *HRaRtX* flows is reduced to 35 kbps, which is a reduction of about 12%. However, this reduction is only 8%, when the same number of flows of the lowest priority class *RaXRe* are entered as shown in Fig. 6 in which the data rate of non-real-time *RaXRe* flows is reduced to provide room for high-priority high-rate *HRaRtX* flows. It gives an insight to the impact of adding new flows of different priority classes. On the other hand, data rate of class *XRtX* is not much affected due to its high priority

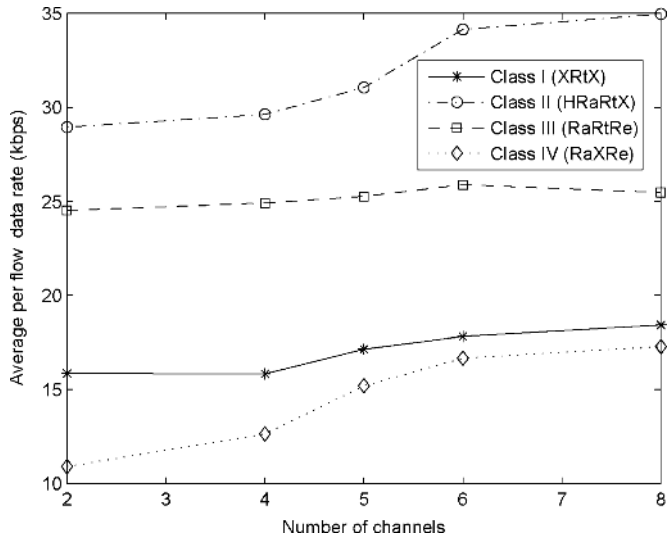

Fig. 7. Average per flow data rate for five flows of each of four traffic classes by varying the number of channels.

with low rate requirement. Although delay in MMSPEED is not higher than the proposed DCA, its data rate is significantly lower for both classes, which is observed to be half as the number of flows are increased to 10. This is due to the fact that MMSPEED is not spectrum-aware and the underlying MAC protocol operates on fixed spectrum that does not cope with the extensive interference in power systems.

The impact of varying the number of data channels under higher traffic load of five flows per each class is shown in Fig. 7. The two real-time and low-rate classes achieve higher rate at smaller channel unlike the other low priority classes but it improves as the number of channels are increased. Hence, DCA framework supports the data rate for each flows corresponding to its class, given that the bandwidth is sufficiently available and maintains the service guarantees in terms of reliability, latency and data rate according to the priority of classes.

VI. Conclusion

This paper presents a cross-layer framework that employs cognitive radio communication to circumvent the hostile propagation conditions in power systems and supports QoS for smart grid applications. The problem is formulated as a *Laypunov* drift optimization with the objective of maximizing the weighted service of traffic flows belonging to different classes. A cross-layer distributed control algorithm (DCA) solution is provided that jointly optimizes the routing, medium access and physical layer functions. Performance results reveal that the increase in number of flows of lower priority class does not affect much of the performance of flows of higher priority classes for their specified attributes. Moreover, under limited number of channels with large PU footprints, presumed to be unwanted signal or noise, each class preserves performance of its flows with respect to its attribute specifications. In addition, performance evaluations show that the increase in number of channels does not necessarily enhance the performance with the same ratio and is limited due to high contention on the common control channel.

REFERENCES

[1] A. Abagnale *et al.*, "Gymkhana: A connectivity-based routing scheme for cognitive radio Ad Hoc networks," in *Proc. IEEE INFOCOM*, 2010, pp. 1–5.

[2] O. B. Akan, O. B. Karli, and O. Ergul, "Cognitive radio sensor networks," *IEEE Network*, vol. 23, no. 4, pp. 34–40, Jul. 2009.

[3] A. Al-Fuqaha *et al.*, "Opportunistic channel selection strategy for better QoS in cooperative networks with cognitive radio capabilities," *IEEE J. Sel. Areas Commun.*, vol. 26, no. 1, pp. 156–167, Jan. 2008.

[4] S. M. Amin and B. F. Wollenberg, "Toward a smart grid: Power delivery for the 21st century," *IEEE Power Energy Mag.*, vol. 3, no. 5, pp. 34–41, Oct. 2005.

[5] A. Bose, "Smart transmission grid applications and their supporting infrastructure," *IEEE Trans. Smart Grid*, vol. 1, no. 1, pp. 11–19, 2010.

[6] K. Chowdhury and M. Felice, "Search: A routing protocol for mobile cognitive radio ad-hoc networks," *Comp. Commun.*, vol. 32, no. 18, pp. 1983–1997, 2009.

[7] K. Chowdhury and I. Akyildiz, "CRP: A routing protocol for cognitive radio ad hoc networks," *IEEE J. Sel. Areas Commun.*, vol. 29, no. 4, pp. 794–804, Apr. 2011.

[8] L. Ding *et al.*, "Cross-layer routing and dynamic spectrum allocation in cognitive radio ad hoc networks," *IEEE Trans. Veh. Technol.*, vol. 59, no. 4, pp. 1969–1979, Apr. 2010.

[9] E. Felemban *et al.*, "Probabilistic QoS guarantee in reliability and timeliness domains in wireless sensor networks," in *Proc. INFOCOM*, 2005, pp. 2646–2657.

[10] L. Georgiadis, M. J. Neely, and L. Tassiulas, "Resource allocation and cross-layer control in wireless networks," *Foundations and Trends in Networking*, vol. 1, no. 1, pp. 1–144, 2006.

[11] V. C. Gungor *et al.*, "A survey on smart grid potential applications and communication requirements," *IEEE Trans. Ind. Inf.*, vol. 9, no. 1, pp. 28–42, Feb. 2013.

[12] V. C. Gungor, B. Lu, and G. P. Hancke, "Opportunities and challenges of wireless sensor networks in smart grid," *IEEE Trans. Ind. Electron.*, vol. 57, no. 10, pp. 3557–3564, Oct. 2010.

[13] V. C. Gungor and D. Sahin, "Cognitive radio networks for smart grid applications: A promising technology to overcome spectrum inefficiency," *IEEE Veh. Technol. Mag.*, vol. 7, no. 2, pp. 41–46, 2012.

[14] V. C. Gungor *et al.*, "Smart grid technologies: Communication technologies and standards," *IEEE Trans. Ind. Inf.*, vol. 7, no. 4, pp. 529–539, Nov. 2011.

[15] H. Li, W. Huang, C. Wu, Z. Li, and F. C. M. Lau, "Utility-maximizing data dissemination in socially selfish cognitive radio networks," in *Proc. IEEE MASS*, 2011, pp. 212–221.

[16] H. Li and W. Zhang, "QoS routing in smart grid," in *Proc. IEEE Globecom*, 2010, pp. 1–6.

[17] M. Lotfinezhad, B. Liang, and E. S. Sousa, "Optimal control of constrained cognitive radio networks with dynamic population size," in *Proc. IEEE INFOCOM*, 2010, pp. 1–9.

[18] M. J. Neely, *Stochastic Network Optimization With Application to Communication and Queueing Systems*. San Francisco, CA, USA: Morgan & Claypool, 2010.

[19] Y. Qiang, J. A. Barria, and T. C. Green, "Communication infrastructures for distributed control of power distribution networks," *IEEE Trans. Ind. Inf.*, vol. 7, no. 2, pp. 316–327, May 2011.

[20] P. Palensky and D. Dietrich, "Demand side management: Demand response, intelligent energy systems, and smart loads," *IEEE Trans. Ind. Inf.*, vol. 7, no. 3, pp. 381–388, Aug. 2011.

[21] T. Sauter and M. Lobashov, "End-to-end communication architecture for smart grids," *IEEE Trans. Ind. Electron.*, vol. 58, no. 4, pp. 1218–1228, Apr. 2011.

[22] G. A. Shah, V. C. Gungor, and O. B. Akan, "A cross-layer design for QoS support in cognitive radio sensor networks for smart grid applications," in *Proc. IEEE ICC*, Jun. 2012, pp. 1378–1382.

[23] Y. Shi *et al.*, "A distributed optimization algorithm for multi-hop cognitive radio networks," in *Proc. IEEE INFOCOM*, 2008, pp. 1292–1300.

[24] P. Siano, C. Cecati, Y. Hao, and J. Kolbusz, "Real time operation of smart grids via FCN networks and optimal power flow," *IEEE Trans. Ind. Inf.*, vol. 8, no. 4, pp. 944–952, Nov. 2012.

[25] W. Sun, X. Yuan, J. Wang, D. Han, and C. Zhang, "Quality of service networking for smart grid distribution monitoring," in *Proc. IEEE SmartGridComm*, 2010, pp. 373–378.

[26] N. H. Tran and C. S. Hong, "Joint rate control and spectrum allocation under packet collision constraint in cognitive radio networks," in *Proc. IEEE Globecom*, 2010, pp. 1–5.

[27] S. Ullo, A. Vaccaro, and G. Velotto, "The role of pervasive and cooperative sensor networks in smart grids communication," in *Proc. IEEE MELECON*, 2010, pp. 443–447.

[28] Q. Yang, J. A. Barria, and T. C. Green, "Communication infrastructures for distributed control of power distribution networks," *IEEE Trans. Ind. Inf.*, vol. 7, no. 2, pp. 316–327, May 2011.

[29] Y. Yang, F. Lambert, and D. Divan, "A survey on technologies for implementing sensor networks for power delivery systems," in *Proc.. IEEE Power Eng. Soc. Gen. Meeting*, 2007, pp. 1–8.

[30] "The network simulator ns-2," The VINT Project, UC Berkeley, LBL, USC/ISI and Xerox PARC [Online]. Available: http://www.isi.edu/nsnam/ns/

Ghalib A. Shah (M'09) received the Ph.D. degree in computer engineering from Middle East Technical University, Ankara, Turkey, in 2007.

He is currently a Visiting Foreign Professor with Al-Khawarizmi Institute of Computer Science, UET Lahore. His research interests include the design and analysis of communication protocols from MAC to Transport layer for cognitive radio networks, wireless multimedia networks, Internet of Things and software defined networks.

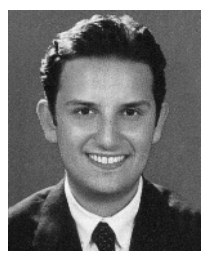

Vehbi C. Gungor (M'02) received th Ph.D. degree in electrical and computer engineering from the Broadband and Wireless Networking Laboratory, Georgia Institute of Technology, Atlanta, GA, USA, in 2007.

Currently, he is an Assistant Professor with the Department of Computer Engineering, Bahcesehir University, Istanbul, Turkey. His current research interests are in smart grid communications, next-generation wireless networks, and wireless ad hoc and sensor networks.

Ozgur B. Akan (M'00–SM'07) received the Ph.D. degree in electrical and computer engineering from the Broadband and Wireless Networking Laboratory, School of Electrical and Computer Engineering, Georgia Institute of Technology, Atlanta, GA, USA, in 2004.

He is currently a Full Professor with the Department of Electrical and Electronics Engineering, Koc University, Istanbul, Turkey, and the Director of the Next-generation and Wireless Communications Lab. His research interests are in wireless communications, nanoscale and molecular communications, and information theory.